

X-RAY DIFFRACTION STUDY AND MODELING OF DAMAGED LAYERS IN $Y_{2.5}Nd_{0.5}Al_5O_{12}$ CERAMICS AFTER SWIFT HEAVY XE IONS IRRADIATION

Nazarov A.A.^{a,*}, P.A. Yunin^a, L.S. Alekseeva^b, A.V. Nokhrin^b

^aInstitute for Physics of Microstructures RAS, Russia, Afonino v., 607680
Academicheskaya str. 7.

e-mail: nazarov.artem@ipmras.ru

^bNational Research Lobachevsky State University of Nizhni Novgorod, Russia,
N. Novgorod, 603022 Gagarina Ave., 23.

Abstract - The paper presents a multiscale modeling of defect formation and latent track generation processes under irradiation of neodymium-doped yttrium-aluminum garnet ceramics with xenon swift heavy ions. The structural characteristics of the material before and after interaction with Xe ions are calculated, and the sizes of the amorphized region of the crystalline matrix are estimated. The theoretical X-ray diffraction pattern is calculated and compared with the experimental one. Good qualitative and quantitative agreement between the calculation results and the experiment is demonstrated, and an interpretation of the X-ray diffraction data is proposed based on the results of molecular dynamics modeling.

INTRODUCTION

Ceramic materials based on mineral-like compounds are promising matrices for the immobilization of radioactive waste [1]. An important characteristic of such materials is their resistance to the irradiation with neutrons, alpha-particles and fission fragments. One of the methods for simulating the effects of fission fragments on a material is its irradiation with swift heavy ions (SHI). It is also important to develop methods for study of structural and phase changes in irradiated samples. One of the most universal and well-studied non-destructive methods for studying the crystal structure of solids is X-ray diffraction analysis (XRD). This method is often used to analyze the phase composition, degree of crystallinity, strain, and radiation resistance in mineral-like ceramic matrices [2-6]. Significant disadvantages of the method are its non-locality and indirectness: a large volume of the sample contributes to the diffraction, and the diffraction data require interpretation within the framework of certain models. Some possibilities of depth-profiling the crystalline properties of the material are provided by the X-ray diffraction analysis in the grazing incidence geometry, however, the problem of constructing a correct model remains. At the same time, Monte Carlo (MC) [7, 8] and molecular dynamics (MD) [9] methods are widely used to model changes in the crystal structure at the atomic level during interaction with projectile particles. Yet, there is a problem of verifying the results of modeling by experiment. In this paper, an approach is proposed to study the processes of defect formation in yttrium-aluminum garnet ceramics under xenon SHI irradiation, based on a combination of MC and MD modeling, calculation of theoretical XRD patterns and their comparison with experimentally measured ones. Such a combination of modeling and experiment simultaneously solves the problem of interpreting XRD data and experimental verification of the proposed models.

EXPERIMENT AND MODELING

The objects of study were $Y_{2.5}Nd_{0.5}Al_5O_{12}$ ceramics, the details of their synthesis and sintering are described in [10]. A detailed experimental characterization of these structures was carried out in [11]. Diffraction patterns of the samples were obtained both in the Bragg-Brentano geometry and at grazing incidence. In the virgin samples, the main

phase of $Y_{2.5}Nd_{0.5}Al_5O_{12}$ (YAG) and the impurity phase of $YAlO_3$ (YAP) were discovered. After irradiation, a phase of strained YAG with an increased lattice parameter is observed (Fig. 1), the diffraction peaks of this phase are shifted relative to the one of the original phases. In this case, the strain value depends on the irradiation fluence. For a more correct analysis and interpretation of experimental data, a multiscale modeling of the interaction process of the SHI with target atoms was carried out in this work.

In the simulation, the atomic structure of a YAG single crystal was set as a target, since the characteristics of the ceramic matrix mostly depend on the behavior of this dominant phase. The energy transfer from the SHI to the YAG electron subsystem was calculated using the TREKIS-3 code [12-14], which implements the MC method. TREKIS includes a number of models describing the electron slowdown of the projectile, allows one to analyze the evolution of the electron subsystem and the subsequent energy transfer to the atomic lattice. As input parameters in TREKIS, the total simulation time was 150 fs, the thickness of the analyzed layer was chosen to be 15 nm, the data were averaged over 1000 iterations of the Monte Carlo calculation, and the final temperature was chosen to be room temperature. The TREKIS calculation is performed in terms of the CDF (complex dielectric function) formalism. The CDF for YAG was calculated by the developers of the TREKIS code and made publicly available; a detailed description of the CDF calculation method is given in [15,16]. The SHI type was 160 MeV Xe.

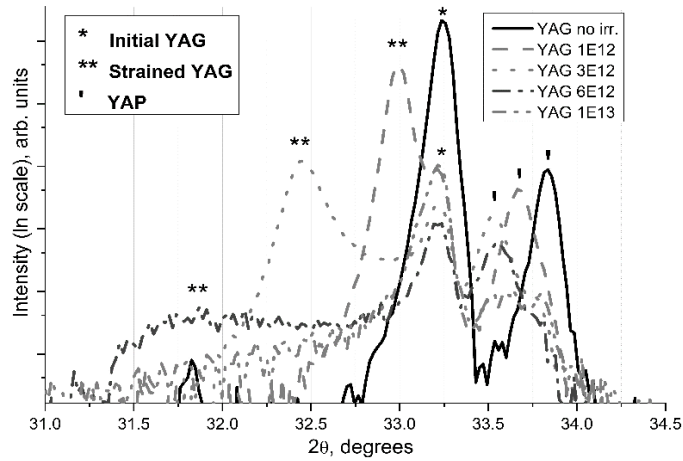


Fig. 1. Fragments of θ - 2θ XRD patterns for YAG samples before and after irradiation with different fluences of SHI.

After modeling in TREKIS, the obtained energy distribution for matrix atoms was imported into LAMMPS [17] as the initial conditions. Then, the MD calculation of the evolution of the atomic system was launched. $Y_3Al_5O_{12}$ supercell with size of $27 \times 27 \times 10$ nm³ and periodic boundary conditions (it means when an atom passes through one side of the unit cell, it re-appears on the opposite side) was set for the calculations in LAMMPS. The classical three-point potential of interatomic interaction was used, which was calculated for YAG in [18], the initial parameter of the unit cell was 12.55 Å. Visualization of the MD modeling results was performed using the OVITO package [19]. To compare and verify the results of modeling by an XRD experiment, theoretical diffraction patterns were calculated for the obtained supercell using the Debyer code [20], which uses the Debye scattering formula [21].

RESULTS AND DISCUSSION

As a result of modeling of Xe SHI interaction with a YAG target in TREKIS-3, the distribution of energy transferred to YAG atoms was obtained (Fig. 2). Starting from the modeling time of ~ 120 fs, the energy changes insignificantly. So it was chosen as an energy distribution that was used as the initial conditions in the subsequent MD modeling. Already at this stage of modeling, the characteristic lateral size of the track can be estimated ~ 10 nm.

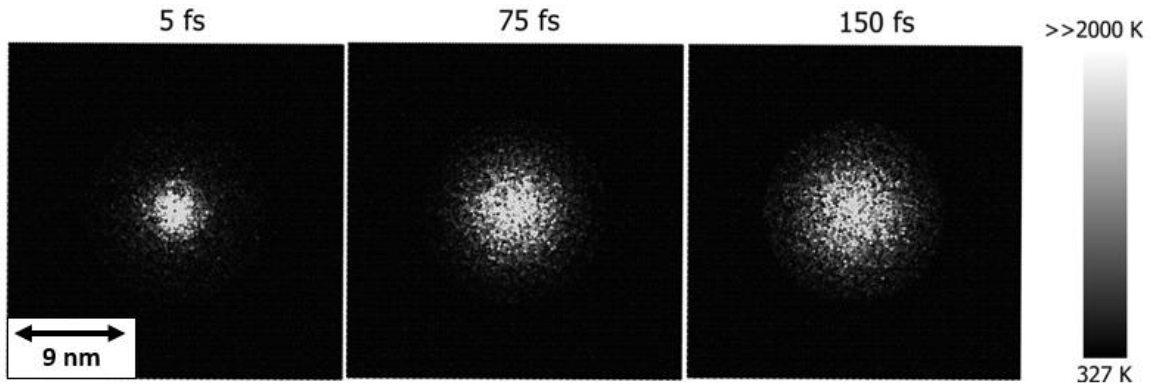


Fig. 2. Visualization of the evolution of the temperature distribution calculated in TREKIS for a YAG simulation cell after 160 MeV Xe impact.

Simulation of relaxation of a heated by Xe SHI YAG supercell with the MD method in LAMMPS allowed visualization of the ion track formation at the atomic level. Complete relaxation of the structure to room temperature occurred within a few nanoseconds. From the simulation results (Fig. 3(a)), one can determine the final track size in the lateral direction of ~ 8 nm. The amorphized core of the track and the strained region of the crystal around the amorphous core are visible. The tint scale in Fig. 3 (a) shows the displacements value of YAG atoms from their initial (before interaction with SHI) positions. It can be seen that the displacement field is non-uniform: there are both regions with a strong displacements and almost unchanged ones.

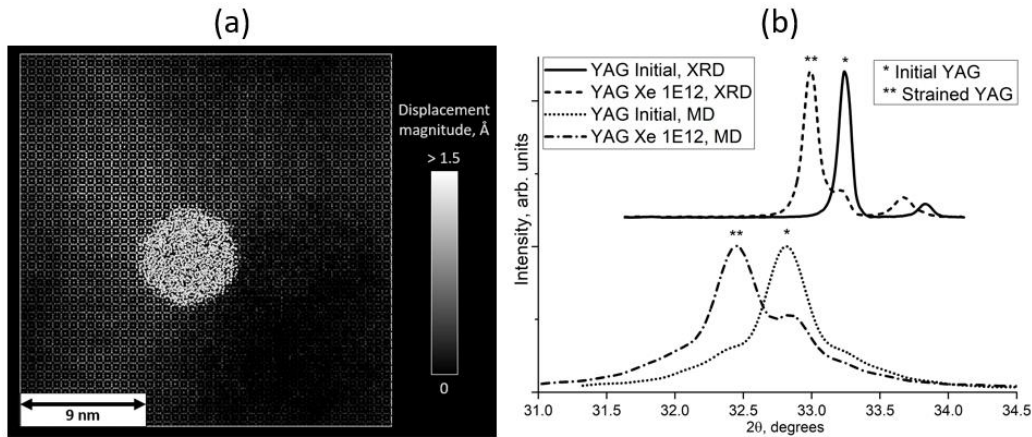


Fig. 3. a. – Atomic displacements distribution in the MD-calculated cell. b. – Calculated end experimental XRD patterns for YAG virgin supercell and supercell after 160 MeV Xe SHI impact.

The diffraction patterns calculated in Debyer for the initial cell before the interaction with the SHI and the cell after the impact are shown in Fig. 3 (b). For the supercell with a track, just as in the experiment, the diffraction peaks of the initial and strained YAG phases are visible. The conditions for impact of one SHI on an area of 15×15 nm quantitatively correspond to the experimental fluence of $\sim 1 \cdot 10^{12} \text{ cm}^{-2}$. Comparing the calculation results with the XRD experiment, we can conclude that the theoretical and experimental diffraction patterns are in good agreement both qualitatively and quantitatively. The constant shift between experimental and calculated diffraction peaks is explained by feature of the chosen interatomic potential. The fraction of the strained phase was estimated from the ratio of peak intensities. In the calculated cell this fraction was 70% of the total cell volume. Estimations for the experimental XRD pattern for fluence of 10^{12} cm^{-2} gave 60% of the strained phase. The lattice strain value of the garnet phase as a result of modeling was 0.8%, while in the experiment for a fluence of 10^{12} cm^{-2} it was 0.6%. A small quantitative discrepancy between the estimates based on modeling and experiment can be explained by a possible overlap of tracks in the experiment, as well as the presence of neodymium impurity, which were not taken into account. Thus, the qualitative and quantitative correspondence between the XRD patterns obtained experimentally and on the basis of multiscale MC&MD modeling confirms the

correctness of the proposed approach. Analysis of the atomic displacement fields after track formation explains the experimental results obtained in [11] and confirms the correctness of the assumptions made about the structure of the YAG near-surface layers after exposure to SHI.

CONCLUSION

The paper demonstrates an approach to studying defect formation processes in YAG ceramics exposed to Xe SHI, based on a combination of MC and MD modeling, calculation of theoretical XRD patterns and their comparison with those measured experimentally. On the one hand, this approach allows one to verify the modeling results, and on the other hand, it offers an interpretation of the XRD experiment results. Qualitative and quantitative agreement was obtained between the modeling and experimental results for YAG ceramics irradiated with Xe SHI. Analysis of the modeled structural changes confirmed the validity of the assumptions made earlier in [11] about the structure of YAG near-surface layers after exposure to SHI. Verification of the proposed research methodology allows it to be used for study of more complex matrices, as well as for predicting the results of radiation tests.

FUNDING

This work was carried out within the state assignment of the Institute for Physics of Microstructures of the Russian Academy of Sciences (FFUF-2024-0042).

ACKNOWLEDGEMENTS

Samples of $Y_{2.5}Nd_{0.5}Al_5O_{12}$ were synthesized and sintered in the Laboratory of Metal Physics of Research Institute of Physics and Technology of the Lobachevsky State University. Irradiation of the ceramic samples with SHI was carried out on the IC-100 cyclotron at Laboratory of Nuclear Reactions of the JINR. MD modeling was performed using the resources of the “Lobachevsky” computing cluster of the Lobachevsky State University. XRD and modeling were carried out in the Laboratory of Diagnostics of Radiation Defects in Solid-State Nanostructures of the Institute for Physics of Microstructures of the Russian Academy of Sciences.

Conflict of interest

The authors of this work declare that they have no conflict of interest.

REFERENCES

1. Koushik Bhandari, V. Grover, P. Kalita, K. Sudarshan, B. Modak, Saurabh K. Sharma, and P. K. Kulriya, Nd^{3+} - $Y_3Al_5O_{12}$ system: Iso-valent substitution driven structural phase evolution and thermo-physical behavior // *Phys. Chem. Chem. Phys.*, 2023, vol. 25, pp. 20495–509.
2. M. E. Karaeva, D. O. Savinykh, A. I. Orlova, A. V. Nokhrin, et al., (Na, Zr) and (Ca, Zr) Phosphate-Molybdates and Phosphate-Tungstates: II–Radiation Test and Hydrolytic Stability // *Materials*, 2023, vol. 16, p. 965.
3. Koushik Bhandari, V. Grover, P. Kalita, K. Sudarshan, et al., Radiation response of $Y_3Al_5O_{12}$ and Nd^{3+} - $Y_3Al_5O_{12}$ to Swift heavy ions: insight into structural damage and defect dynamics // *Phys. Chem. Chem. Phys.*, 2023, vol. 25, pp. 20495–509.
4. P. A. Yunin, A. A. Nazarov, and E. A. Potanina, Application of the GIXRD Technique to Investigation of Damaged Layers in $NaNd(WO_4)_2$ and $NaNd(MoO_4)_2$ Ceramics Irradiated with High-Energy Ions // *Tech. Phys.*, 2024, vol. 69, pp. 442–46.
5. A.J. London, B.K. Panigrahi, C.C. Tang, C. Murray, and C.R.M. Grovenor, Glancing angle XRD analysis of particle stability under self-ion irradiation in oxide dispersion strengthened alloys // *Scripta Materialia*, 2016, vol. 110, pp. 24–27.

6. P. V. Andreev, P. D. Drozhilkin, L. S. Alekseeva, et al., Physical and Mechanical Properties of Ceramics Based on Si₃N₄ of Various Dispersion with 3% Y₂O₃–Al₂O₃ // *Inorg. Mater. Appl. Res.*, 2024, vol. 15, pp. 470–79.
7. James F. Ziegler, M.D. Ziegler, and J.P. Biersack, SRIM – The stopping and range of ions in matter (2010) // *Nuclear Instr. and Methods in Phys. Res. Section B: Beam Interactions with Materials and Atoms*, 2010, vol. 268, pp. 1818–23.
8. R.E. Stoller, M.B. Toloczko, G.S. Was, A.G. Certain, S. Dwaraknath, F.A. Garner, On the use of SRIM for computing radiation damage exposure // *Nuclear Instruments and Methods in Physics Research Section B: Beam Interactions with Materials and Atoms*, 2013, vol. 310, pp 75-80.
9. M.W. Ullah, A. Kuronen, F. Djurabekova, et al., Defect clustering in irradiation of GaN by single and molecular ions // *Defect clustering in irradiation of GaN by single and molecular ions // Vacuum*, 2014, vol. 105, pp. 88–90.
10. L.S. Golovkina, A.I. Orlova, A.V. Nokhrin, et al., Spark Plasma Sintering of fine-grain ceramic-metal composites based on garnet-structure oxide Y_{2.5}Nd_{0.5}Al₅O₁₂ for inert matrix fuel // *Materials Chemistry and Physics*, 2018, vol. 214, pp. 516–26.
11. L.S. Alekseeva, A.V. Nokhrin, P.A. Yunin, A.A. Nazarov, et al., Radiation resistance of fine-grained YAG:Nd ceramics irradiated with swift heavy multi-charged Ar and Xe ions // *Ceramics International*, 2024.
12. R A Rymzhanov, N Medvedev, and A E Volkov, Damage threshold and structure of swift heavy ion tracks in Al₂O₃ // *J. Phys. D: Appl. Phys.*, 2017, vol. 50, p. 475301.
13. R.E. Stoller, M.B. Toloczko, G.S. Was, et al., On the use of SRIM for computing radiation damage exposure // *Nuclear Instruments and Methods in Physics Research Section B: Beam Interactions with Materials and Atoms*, 2013, vol. 310, pp. 75–80.
14. N. Medvedev, A. E. Volkov, R. Rymzhanov, et al., Frontiers, challenges, and solutions in modeling of swift heavy ion effects in materials // *Journal of Applied Physics*, 2023, vol. 133.
15. N. A. Medvedev, R. A. Rymzhanov, and A. E. Volkov, Time-resolved electron kinetics in swift heavy ion irradiated solids // *J. Phys. D: Appl. Phys.*, 2015, vol. 48, p. 355303.
16. R.A. Rymzhanov, N.A. Medvedev, and A.E. Volkov, Effects of model approximations for electron, hole, and photon transport in swift heavy ion tracks // *Nuclear Instruments and Methods in Physics Research Section B: Beam Interactions with Materials and Atoms*, 2016, vol. 388, pp. 41–52.
17. Steve Plimpton, Fast Parallel Algorithms for Short-Range Molecular Dynamics // *Journal of Computational Physics*, 1995, vol. 117, pp. 1–19.
18. AlDosari, M. S. Thermal properties of yttrium aluminum garnet from molecular dynamics simulations // *Vanderbilt University*, 2012.
19. Alexander Stukowski, Visualization and analysis of atomistic simulation data with OVITO—the Open Visualization Tool. Model // *Modelling Simul. Mater. Sci. Eng.*, 2009, vol. 18, p. 015012.
20. Marcin Wojdyr, Sarah Khalil, Yun Liu, and Izabela Szlufarska, Energetics and structure of $\langle 001 \rangle$ tilt grain boundaries in SiC // *Modelling Simul. Mater. Sci. Eng.*, 2010, vol. 18, p. 075009.
21. P. Debye: *Annalen Der Physik, Zerstreung von Röntgenstrahlen* // 1915, vol. 351, pp. 809–23.